

Ventral Striatal Network Connectivity Reflects Reward Learning and Behavior in Patients with Parkinson's Disease

Kalen Petersen ^{1,2}, Nelleke Van Wouwe,¹ Adam Stark,² Ya-Chen Lin,³ Hakmook Kang,³ Paula Trujillo-Diaz,² Robert Kessler,⁴ David Zald,⁵ Manus J. Donahue,^{1,2} and Daniel O. Claassen^{1,2*}

¹Department of Radiology, Vanderbilt University Medical Center, Nashville, Tennessee

²Department of Neurology, Vanderbilt University Medical Center, Nashville, Tennessee

³Department of Biostatistics, Vanderbilt University Medical Center, Nashville, Tennessee

⁴Department of Radiology, University of Alabama School of Medicine, Birmingham, Alabama

⁵Department of Psychology, Vanderbilt University, Nashville, Tennessee

Abstract: A subgroup of Parkinson's disease (PD) patients treated with dopaminergic therapy develop compulsive reward-driven behaviors, which can result in life-altering morbidity. The mesocorticolimbic dopamine network guides reward-motivated behavior; however, its role in this treatment-related behavioral phenotype is incompletely understood. Here, mesocorticolimbic network function in PD patients who develop impulsive and compulsive behaviors (ICB) in response to dopamine agonists was assessed using BOLD fMRI. The tested hypothesis was that network connectivity between the ventral striatum and the limbic cortex is elevated in patients with ICB and that reward-learning proficiency reflects the extent of mesocorticolimbic network connectivity. To evaluate this hypothesis, 3.0T BOLD-fMRI was applied to measure baseline functional connectivity on and off dopamine agonist therapy in age and sex-matched PD patients with ($n = 19$) or without ($n = 18$) ICB. An incentive-based task was administered to a subset of patients ($n = 20$) to quantify positively or negatively reinforced learning. Whole-brain voxelwise analyses and region-of-interest-based mixed linear effects modeling were performed. Elevated ventral striatal connectivity to the anterior cingulate gyrus ($P = 0.013$), orbitofrontal cortex ($P = 0.034$), insula ($P = 0.044$), putamen ($P = 0.014$), globus pallidus ($P < 0.01$), and thalamus ($P < 0.01$) was observed in patients with ICB. A strong trend for elevated amygdala-to-midbrain connectivity was found in ICB patients on dopamine agonist. Ventral striatum-to-subgenual cingulate connectivity correlated with reward learning ($P < 0.01$), but not with punishment-avoidance learning. These data indicate that PD-ICB patients have elevated network connectivity in the mesocorticolimbic network. Behaviorally, proficient reward-based learning is related to this enhanced limbic and ventral striatal connectivity. *Hum Brain Mapp* 39:509–521, 2018. © 2017 Wiley Periodicals, Inc.

Additional Supporting Information may be found in the online version of this article.

Prepared for submission as an original article in Human Brain Mapping

Contract grant sponsor: NIH/NINDS; Contract grant numbers: R01 NS097783 and K23 NS080988; Contract grant sponsor: American Heart Association; Contract grant number: 14GRNT20150004; Contract grant sponsor: Clinical translational science award (National Center for Advancing Translational Sciences); Contract grant number: UL1TR000445

*Correspondence to: Daniel O. Claassen, Village at Vanderbilt, 1500 21st Ave. S., Suite 3000, Nashville, TN 37212. E-mail: daniel.claassen@vanderbilt.edu

Received for publication 20 September 2017; Accepted 16 October 2017.

DOI: 10.1002/hbm.23860

Published online 31 October 2017 in Wiley Online Library (wileyonlinelibrary.com).

Key words: Parkinson's disease; impulse control disorder; connectivity; BOLD; MRI

INTRODUCTION

Motor symptoms in patients with Parkinson's disease (PD) improve with dopamine replacement therapy, but patients can develop debilitating reward-driven impulsive and compulsive behaviors (ICB). Dopamine agonist (DAA) use in particular is the greatest risk factor for this behavior, where prevalence estimates indicate ~15% of patients on DAA therapy develop these symptoms [Weintraub et al., 2015]. Consequent maladaptive activities include hypersexuality, compulsive gambling, shopping, and binge eating [American Psychiatric Association, 2013; Perez-Lloret et al., 2011].

Medication effects likely target the mesocorticolimbic incentive-learning network, an integrated system of cortical and subcortical structures in which the ventral striatum plays a central role [Haber and Behrens, 2014]. More specifically, the ventral striatum receives dopaminergic projections from the ventral tegmental area of the midbrain, and mediates behavior-reinforcing effects of rewarding activities. Analogous to the nucleus accumbens in lower order species, the ventral striatum is important in motivation and reward-associative learning [Ikemoto and Panksepp, 1999; Olds and Milner, 1954] and is consistently implicated in drug addiction [Pierce and Kumaresan, 2006].

Additionally, the amygdala, traditionally identified with associative learning involving fear or negative emotional valence, is a key mesolimbic structure. The amygdala encodes affective and motivational significance to rewarding events, mediates reward-learning [Tye et al., 2008], and interacts with the ventral striatum dopamine system to connect reward-association effects with behavior [Cador et al., 1989]. While these structures have been studied extensively in the context of normal function and disease states, the behavioral outcomes of dopaminergic therapy for PD patients present a unique opportunity to investigate pathological activity in these networks, and related behavior, under differing pharmacologic conditions.

In this context, the effect of DAA-linked ICB on functional neural networks remains poorly understood. It is unclear why a subset of individuals receiving DAA therapy develop these altered behaviors. As DAAs show a preference for D2-like receptors, which localize to the ventral striatum and mediate its activity [Claassen et al., 2017; Murray et al., 1994], altered connectivity within this region to other mesocorticolimbic structures may have relevance. A clearer understanding of circuits that may be altered in patients with these behaviors could inform better clinical practices to mitigate the impact of these side effects.

It is unknown whether DAAs produce ICB by directly reshaping brain connectivity, or by acting upon pre-existing group differences in network activity. Only one previous study examined striatal functional connectivity in PD-ICB patients [Carriere et al., 2015] and found functional disconnection in striato-cortical circuits. However, this study did not evaluate on and off medication states nor did it examine connectivity between subcortical structures (rather than exclusively between the basal ganglia and cortical surface) or include the amygdala.

As ICB manifestations are often categorized as behavioral addictions [Dagher and Robbins, 2009; Voon and Fox, 2007], we hypothesized that DAA-treated PD patients with this behavioral phenotype have increased functional connectivity between the ventral striatum and components of the limbic striato-pallido-thalamo-cortical loop, including pathways to the anterior cingulate gyrus and orbitofrontal cortex. To test this hypothesis, we applied pharmacological baseline blood oxygenation level-dependent (BOLD) fMRI to measure regional connectivity of the hemodynamic signal between the ventral striatum and mesocorticolimbic regions implicated in incentive salience, motivation, and addiction. Because amygdala activity has also been linked with reward-motivated behaviors [Hitchcott et al., 1997; Murray, 2007] on and off DAA, we additionally examined amygdala connectivity with reward network components. Finally, since striato-

Abbreviations

BOLD	blood oxygenation level-dependent
COMPCOR	component-based noise correction
DAA	dopamine agonist
FDR	false discovery rate
fMRI	functional magnetic resonance imaging
FSL	FMRIB software library
FWHM	full width at half-maximum
IBASPM	individual brain atlases using statistical parametric mapping software
ICB	impulsive and compulsive behaviors
LASSO	least absolute shrinkage and selection operator
MDS-UPDRS	Movement Disorders Society-United Parkinson's Disease Rating Scale
MELODIC	multivariate exploratory linear optimized decomposition into independent components
MNI	Montreal neurological institute
MPRAGE	magnetization prepared rapid gradient echo
PD	Parkinson's disease
QUIP-RS	Questionnaire for Impulsive-Compulsive Disorders in Parkinson's Disease-Rating Scale
ROI	region of interest
SENSE	sensitivity encoding
SPM	statistical parametric mapping
TE	echo time
TI	inversion time
TR	repetition time

TABLE I. Subject demographics and behavioral and cognitive traits

Variable	PD ICB-	PD ICB+	P-value
N	18	19	
Gender (Male/Female)	13/5	12/7	
Age (years)	62.7 ± 10.1	61.0 ± 7.1	0.56
Disease Duration (years)	6.1 ± 4.5	6.2 ± 3.7	0.91
CES-D	15.1 ± 7.2	17.4 ± 11.2	0.46
MDS-UPDRS Part II	23.2 ± 7.7	22.3 ± 9.6	0.75
QUIP-RS Total	18.9 ± 11.1	35.9 ± 9.7	<0.001 ^a
ICB Symptom Distribution (based on semi-structured behavioral interview)			
Hobbyism	0/19	12/19	
Eating	0/19	13/19	
Sex	0/19	12/19	
Shopping	0/19	4/19	
Gambling	0/19	0/19	
Dopamine Replacement Therapy			
Total LEDD (mg/day)	609.8 ± 390.3	639.1 ± 417.1	0.82
Agonist Single Dose Equivalent (mg/day)	103.9 ± 65.1	117.6 ± 73.7	0.47

Values reported as mean ± one standard deviation or fractions of subjects.

^aMeets significance criteria of two-sided $P < 0.05$.

cortical networks are implicated in action choice and reward valuation [Bogacz and Gurney, 2007; Tanaka et al., 2004], we tested whether functional connectivity was linked to differences in incentive-based learning. To our knowledge, this is the first study to test ICB-related connectivity differences while modeling controlled on-DAA and off-dopaminergic medication states.

MATERIALS AND METHODS

Demographics

Patients with PD ($n = 37$; gender = 12F/25M; age = 61.8 ± 8.4 years) were recruited from the Vanderbilt University Movement Disorders Clinic and provided informed, written consent for this prospective study. Participants met the following inclusion criteria: no history of (1) non-PD-related neurological disease; (2) psychiatric disease including bipolar affective disorder, schizophrenia, or other condition known to compromise executive cognitive functions; (3) moderate-to-severe depression, based on the Center for Epidemiological Studies Depression Scale-Revised; (4) medical conditions known to interfere with cognition (e.g., diabetes, pulmonary disease), and (5) confounding medical therapies such as antipsychotics or acetylcholinesterase inhibitors. All participants reported stable mood functioning, absence of major depression, and did not meet clinical criteria for mild cognitive impairment or dementia based on a neurological exam.

Classification, Cognitive, and Motor Testing

Patients completed the Questionnaire for Impulsive-Compulsive Disorders in Parkinson's Disease-Rating Scale (QUIP-RS). To measure PD severity, a clinical examination

was administered by a board-certified neurologist (D.O.C.). The Movement Disorders Society-United Parkinson's Disease Rating Scale (MDS-UPDRS) part II [Goetz et al., 2008] was used to assess self-reported disease severity. Patients' current prescribed dosages of dopaminergic medication, including Levodopa and DAAs, were converted to levodopa equivalent daily dosage (LEDD) [Tomlinson et al., 2010]. Patients were categorized as ICB+ ($n = 19$) or ICB- ($n = 18$) according to previous methods [Weintraub, 2009] based on a structured behavioral interview with the patient and spouse. ICB+ patients were defined as those exhibiting one or more of the following behaviors that emerged after the initiation of DAA medication: compulsive eating, compulsive gambling, compulsive shopping, hypersexuality, and compulsive hobbyism. In this sample, most commonly encountered problematic behaviors were hypersexuality and compulsive eating (Table I); no patients exhibited compulsive gambling. ICB- patients served as the control group, since the object was to identify ICB-specific (rather than PD-specific) connectivity patterns.

Patients were required to refrain from taking all dopaminergic medications prior to the off-dopamine therapy scan (16 h Levodopa-free, 36 h DAA-free, due to differential drug kinetics) to reduce circulating drugs and abrogate residual drug effects. For the on-DAA scan, patients took their prescribed DAA dosage (but not levodopa) such that the clinical testing and exam were performed in the on-DAA-only state.

Incentive Learning

A subset of participants ($n = 8$ ICB+; $n = 12$ ICB-) completed an action-valence learning task, both on-DAA and off-dopamine. Participants were exposed to new stimuli in each visit, so each session required new learning. Stimulus

TABLE II. Optimal response for each of the four action-valence combinations (Stimulus A to D)

	Reward	Punishment avoidance
Action	Act to gain reward (A)	Act to avoid punishment (C)
Inaction	Withhold to gain reward (B)	Withhold to avoid punishment (D)

order within each session was randomized. Supporting Information Fig. S2 depicts two example trials of the action-valence learning task. For a detailed description of the trials, see Van Wouwe et al. [2017]. Subjects were instructed that the goal of this task was to learn to act or withhold action in response to each of four cartoon characters to maximize earnings by gaining rewards (+25 cents) and avoiding losses (i.e., punishments, -25 cents).

Unbeknownst to the subjects, two of the cartoon characters provided outcomes that were rewarded or unrewarded, and the other two cartoon characters provided outcomes that were either punished or unpunished. Thus, the former two characters were associated with reward learning, whereas the latter two characters were associated with punishment avoidance learning. In addition, unknown to the subject, one character from each set of two produced the optimal outcome (i.e., either gain reward or avoid punishment) when the subject acted, but the other character from each set produced the optimal outcome when the subject withheld action.

This setup orthogonalized both reward/punishment valence and action/inaction. Table II provides a summary with the optimal response for each condition. The optimal response was probabilistically rewarded (A and B), or not punished (C and D) 80% of the time, whereas the nonoptimal response always yielded the undesired outcome (either no reward in A and B or a punishment in condition C and D). Subjects were unaware of the exact probabilities of each action-outcome association, but they were instructed that each action associated with a particular stimulus would lead to a particular outcome most of the time, but not always. Before the actual experiment, participants performed 15 practice trials during which they experienced the probabilistic nature of the task.

Subjects completed 160 learning trials, divided into four 40-trial blocks. Accuracy was defined by the percentage of trials in which the subject selected the optimal response. To confirm that participants learned throughout the task, performance across the four learning blocks was first analyzed. Subsequent analyses were performed on the final block, reflecting asymptotic maximum learning.

MRI Acquisition

Scans were performed at 3 Tesla (3.0 T) in separate on-DAA and off-dopamine conditions using a Philips Achieva scanner (Philips Healthcare, Best, The Netherlands) with

body coil transmission and 8-channel SENSE array head coil reception. The multimodal imaging protocol included a standard T_1 -weighted anatomical (3D MPRAGE; spatial resolution = $1 \times 1 \times 1 \text{ mm}^3$; TR/TE = 8.9/4.6 ms), T_2 -weighted FLAIR (3D T_2 -weighted turbo-spin-echo; spatial resolution = $1 \times 1 \times 1 \text{ mm}^3$; TR/TI/TE = 4,000/2,800/120 ms), and BOLD (spatial resolution = $3.5 \times 3.5 \times 3.5 \text{ mm}^3$; single shot gradient echo echo planar imaging; TR/TE = 2,000/35 ms; flip angle = 75° , duration = 5 min). The BOLD field-of-view was $224 \times 224 \times 122.5 \text{ mm}$ (matrix size = $64 \times 64 \times 35$) and was oriented to have a 30° angle between the anterior commissure – posterior commissure line and the plane of the imaging volume (chosen to reduce the spatial extent of phase heterogeneity and signal dropout beyond lower frontal lobe voxels). The slice acquisition order was interleaved ascending.

Voxelwise Analysis

Image preprocessing was performed using standard routines from the FMRIB software library (FSL) [Smith et al., 2004]. The first three volumes of each scan were removed to ensure the signal was at steady-state, leaving 147 frames. Next, BOLD scans were motion-corrected by registration to the central frame, slice-time corrected, spatially smoothed with a Gaussian kernel [full-width-half-maximum (FWHM) = 5 mm], and bandpass filtered to exclude frequencies below 0.01 Hz (scanner drift) and above 0.15 Hz (high-frequency nuisance fluctuations).

Next, to reduce contributions from residual motion and nuisance fluctuations, a conservative data-driven approach similar to COMPCOR [Behzadi et al., 2007] was applied. Here, FSL MELODIC was used to decompose the voxelwise timecourses into 25 independent components. Next, *fsl_regfilt* was applied to regress out components found to be artifactual using the following criteria (1) no resemblance to known functional networks, for example, those described in [Smith et al., 2009] or (2) localization to the skull. Examples of components are shown in Supporting Information Figure S1 for a representative subject. Nuisance regressors were selected to remove a similar percentage of explained variance in all subjects and variance removed was similar between ICB groups (ICB+: 27.3%; ICB-: 25.2%; not significant in a two-tailed t-test).

Next, anatomical T_1 -weighted images were skull-stripped and automatically segmented and seed regions in ventral striatum and amygdala were defined by FSL FIRST outputs [Patenaude et al., 2011] (Fig. 1A). All seed regions were bilateral. T_1 -space masks were examined by a board-certified neurologist (D.O.C) and neuroradiologist (R.K.) to confirm that the segmentation was representative of the structure. Seed region masks were then transformed to the BOLD scans and used to extract the seed timecourses from the pre-processed BOLD images. This procedure was used to reduce confounds in which timecourses are modified as a result of coregistration and resampling. The use of

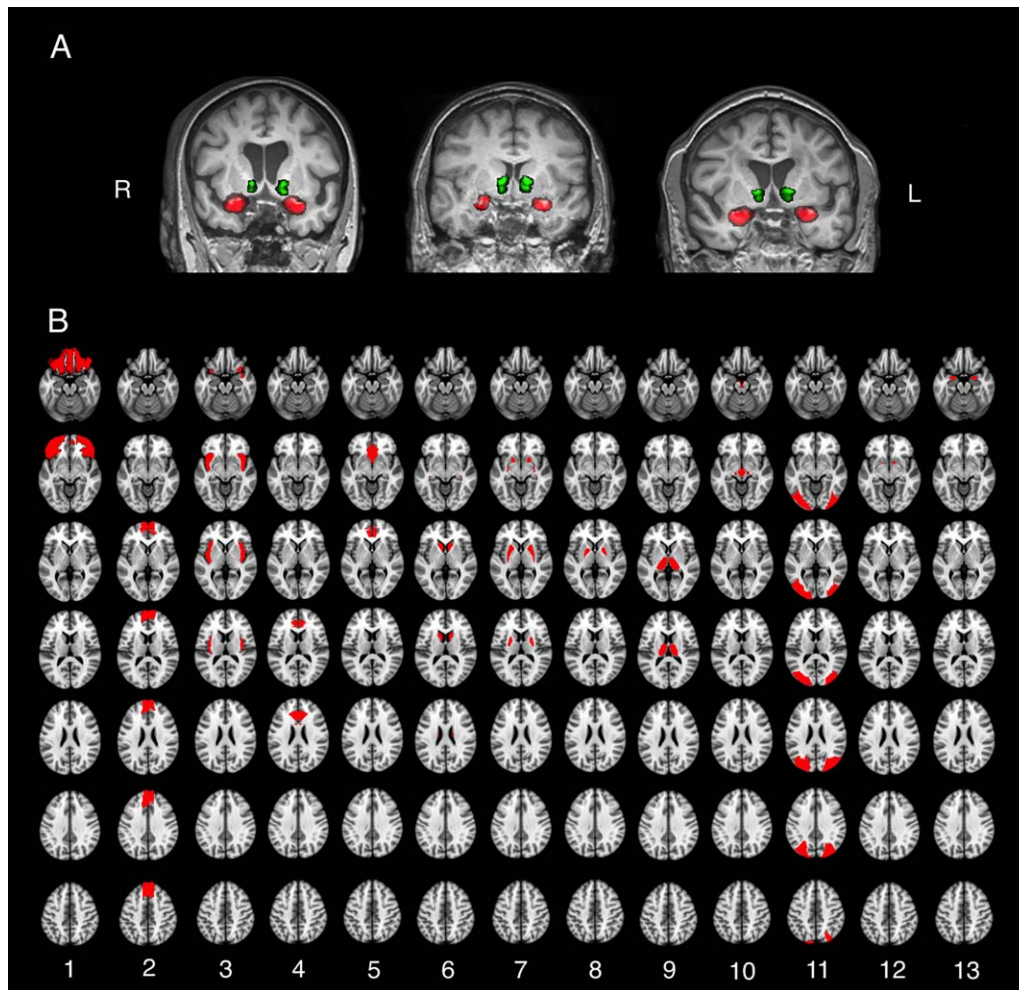


Figure 1.

A, Representative seed regions determined by FSL-FIRST. Green: ventral striatum; red: amygdala. **B**, All mesocorticolimbic ROIs used in group-level analysis. ROIs were defined using the IBASPM116 segmentation tool implemented in the WFU pick-atlas Matlab toolbox. Orbitofrontal cortex (1), ventromedial

prefrontal cortex (2), insula (3), dorsal anterior cingulate gyrus (4), subgenual anterior cingulate (5), caudate (6), putamen (7), globus pallidus (8), thalamus (9), midbrain (10), occipital lobe (11), ventral striatum (for amygdala seed) (12), and amygdala (for ventral striatum seed) (13).

subject-derived seed masks reduces confounding partial volume effects due to variability in shape, size, and relative position of brain structures that are difficult to account for when using standard space atlases, but are common in older patients with neurodegeneration [Cherubini et al., 2009; Zhang et al., 2014].

Next, subject-level connectivity modeling was performed using FSL-FEAT. Seed timecourses were used as explanatory variables in a voxelwise linear regression in native space. Each voxel's z-statistic was calculated using Fisher's z-transform. Subject-level connectivity maps were registered to native T_1 space and subsequently to the 2-mm Montreal Neurological Institute (MNI) 152 standard brain atlas. These MNI-space connectivity z-statistic maps were then used as inputs in a group-level analysis.

To determine whether regions outside of the mesocorticolimbic network are differently connected with the ventral striatum or amygdala in ICB patients, a group-level analysis was performed using voxelwise statistics in standard space using Statistical Parametric Mapping (SPM), with familywise error rate correction for multiple comparisons. Explanatory variables were ICB status (+/-) and drug status (on-DAA/off-dopamine). Age was treated as a covariate of no interest.

Region of Interest (ROI)-Based Analysis

Image preprocessing for the ROI-based analysis was identical to methods in voxelwise analysis, except in two

respects. First, a smaller spatial smoothing kernel was applied (FWHM = 3 mm), as the ROI-based approach did not require as high a signal-to-noise ratio, and the goal was to avoid partial volume effects between the ventral striatum and lateral ventricles; 3–5 mm spatial smoothing is used routinely in fMRI analyses. Secondly, global signal regression was used rather than data-driven denoising in this analysis to ensure that voxelwise results were not due to bias in the selection of noise components. To extract global signal, whole-brain masks were created using FSL BET applied to the motion-corrected fMRI image. Global signal was then included as an additional regressor of no interest to account for residual motion effects and spatially nonspecific physiological noise.

ROI-based connectivity analysis was performed using a mixed-effects linear model implemented in R Statistical Software version 3.3.2 (Foundation for Statistical Computing). Explanatory variables were ICB status (+/-), drug status (on-DAA/off-dopamine), and drug-ICB interaction. Twelve target ROIs were tested, as motivated by our study hypotheses: orbitofrontal cortex, ventromedial prefrontal cortex, insula, dorsal anterior cingulate gyrus, subgenual anterior cingulate gyrus (inferior to the genu of the corpus callosum), caudate, putamen, globus pallidus, thalamus, midbrain (ventral tegmental area and substantia nigra), occipital lobe (negative control), and ventral striatum (for the amygdala seed) or amygdala (for the ventral striatum seed; Fig. 1B). ROIs were defined using the Wake Forest University (WFU) pick-atlas tool IBASPM116 definitions [Maldjian, 1994]. All target ROIs were bilateral.

Statistical Analysis and Hypothesis Testing

Continuous measurements of patient demographics (Table I) were compared between groups using the Mann-Whitney *U* test.

Hypothesis 1, that ICB+ individuals would exhibit increased ventral striatal connectivity with reward network components while on DAA, was tested using both a voxelwise analysis with familywise error rate correction and an ROI-based approach with false discovery rate (FDR) correction. For the ROI analysis, a mixed-effects linear model was employed since the assumption of independence in a general linear model was violated by repeated measurements (on- and off-drug scans). Connectivity differences were considered significant at FDR = 0.10, a threshold recommended by Benjamini [Benjamini and Hochberg, 1995; Genovese et al., 2002]. The voxelwise parametric analysis was performed using multiple regression with ICB group and drug status as covariates of interest, and age as a covariate of no interest. Voxels were thresholded at $P < 0.001$. Clusters were considered significant at family wise error corrected $P < 0.05$.

To test Hypothesis 2 that while on-DAA, ICB+ patients exhibit elevated reward-based learning, but not punishment avoidance-based learning, a mixed ANOVA was

performed, with three within-subject factors; Action (action, inaction), Valence (reward, punishment avoidance), Medication (on-DAA, off-dopamine); and one between-subjects factor, Group (ICB+, ICB-).

To test Hypothesis 3 that ventral striatal connectivity relates to incentive learning, ventral striatal connectivity values with mesocorticolimbic ROIs were used as independent variables in least absolute shrinkage and selection operator (LASSO) regressions, where task score was the dependent variable. LASSO regression performs variable selection to determine what covariates are important in explaining the dependent variable, setting less-important terms to zero [Tibshirani, 1996]. This analysis included ICB group status as a covariate, since reward scores were different between groups, and collapsed across drug status, since the goal was to compare connectivity and reward learning independent of drug effects. LASSO regression was performed using the glmnet package [Friedman et al., 2010] and bootstrapped in R. LASSO regression was performed with two different datasets: reward vs. ventral striatum connectivity, and punishment versus ventral striatum connectivity. In each regression, ICB status was included as a nonpenalized explanatory variable (i.e., controlled for). The LASSO regression was performed on 500 bootstrap samples per condition, and the number of times each seed-target pair was chosen reported. Seed-target pairs were considered highly important if they were chosen in 80 percent or more bootstraps. For any seed-target pairs thus categorized, Spearman's ρ was calculated.

RESULTS

Demographics

Table I summarizes non-imaging study values. ICB+ and ICB- groups were matched ($P > 0.05$) for age, disease severity (UPDRS part II), depression (CES-D), disease duration, and dosage (LEDD or DAA single dose equivalent). QUIP-RS was significantly greater for ICB+ patients after correction for multiple comparisons ($P < 0.001$).

Hypothesis 1: Network Connectivity in PD-ICB

The voxelwise analysis and ROI-based analysis yielded largely consistent results. In the voxelwise approach, we found increased ventral striatal connectivity with two significant clusters in ICB+ patients. Cluster 1 extended from the right thalamus through the basal ganglia (esp. globus pallidus and putamen) into the subgenual anterior cingulate gyrus as well as lateral orbitofrontal and dorsolateral prefrontal cortex. Cluster 2 mirrored cluster 1 in the left prefrontal cortex (Fig. 2).

In the ROI-based analysis, the ventral striatum of ICB+ patients exhibited increased connectivity with dorsal anterior cingulate gyrus ($P = 0.013$), orbitofrontal cortex

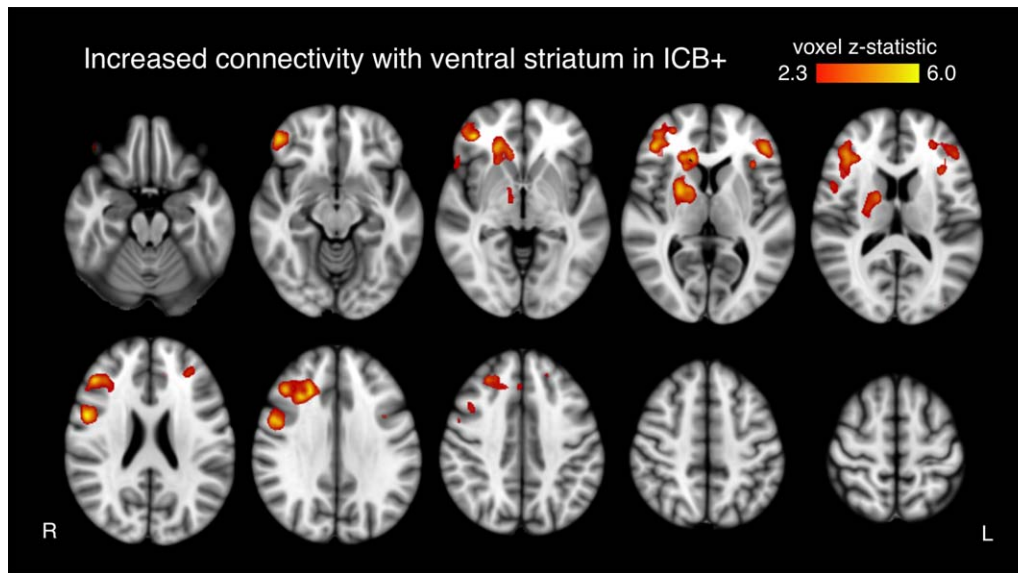


Figure 2.

Effects of ICBs on voxelwise connectivity. Ventral striatum connectivity between ICB groups. No DAA effect was observed. Only clusters significant after family wise error correction are shown.

($P = 0.034$), insula ($P = 0.044$), putamen ($P = 0.014$), globus pallidus ($P < 0.01$), and thalamus ($P < 0.01$; all reported P -values significant after FDR correction; Fig. 3A). No main effect was observed for drug. An ICB-drug interaction effect between the amygdala and the midbrain was observed, such that off-dopamine, ICB+ status is associated with decreased connectivity, but on-DAA, ICB+ status is associated with increased connectivity. This effect was individually significant, but was not significant after FDR correction ($P = 0.011$; Fig. 3B).

Hypothesis 2: Incentive Learning

All patients showed an increase in learning across blocks, both on- and off-medication (off-dopamine, $P < 0.001$; on-DAA, $P < 0.002$). Figure 4 displays the accuracy for each action-valence condition, comparing ICB+ and ICB- in each medication state. Learning proficiency was higher on average in ICB+ patients (91% correct responses) than in ICB- patients (79%; $P < 0.01$). There were no significant main effects of Medication or Action, nor any significant interaction between these two factors. Based on our hypothesis that ICB+ patients will particularly excel at learning from rewards, we compared reward and punishment learning (across medication states and action-learning conditions) separately between ICB groups. Reward learning was more proficient ($P < 0.01$) in ICB+ patients (90%) compared with the ICB- patients (73%). ICB+ patients also tended to be more proficient on punishment avoidance learning (93%) than the ICB- patients (84%), but this did not meet significance criteria ($P = 0.07$).

Supporting Information File 1 contains all individual task scores and connectivity values used in this analysis.

Hypothesis 3: Network Connectivity and Incentive Learning

Ventral striatum connectivity was tested for a relationship with incentive learning. This analysis controlled for ICB status, since learning scores were different between ICB groups. For reward score, ventral striatum to subgenual cingulate was highly important, chosen in the LASSO regression in 91% of bootstrapped samples. Ventral striatum to subgenual anterior cingulate connectivity was positively correlated with reward learning performance ($\rho = 0.43$, $P < 0.01$). No other seed-target connectivity pair exceeded the 80% threshold, nor did any regions exceed this threshold for punishment avoidance. Table III summarizes LASSO regression results.

DISCUSSION

In this study, we ask: are mesocorticolimbic networks altered in patients with medication-induced impulse control disorder? We used baseline fMRI to test for altered brain connectivity in impulsive and compulsive individuals and found heightened connectivity between the ventral striatum and the limbic loop to the anterior cingulate gyrus and orbitofrontal cortex, as well as to other limbic structures. We found evidence in support of the strength of this connection relating to reward-based learning.

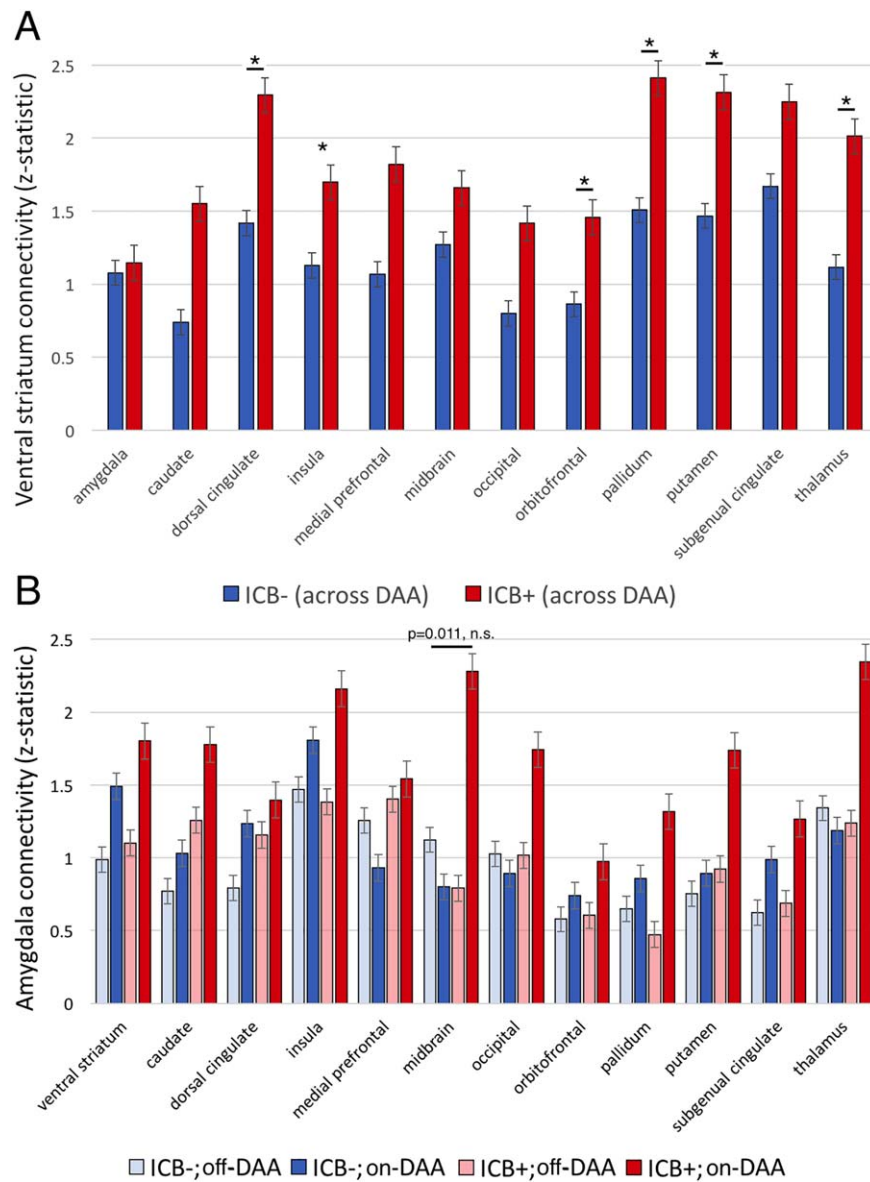


Figure 3.

Effects of ICBs on ROI-based connectivity. Connectivity differences between ICB and DAA groups. **A**, Ventral striatum connectivity between ICB groups. No DAA effect was observed. Asterisk indicates seed-target pairs significant after multiple

comparisons correction. **B**, Amygdala connectivity among ICB groups and drug states. Bar with *P*-value represents a DAA-ICB interaction effect not significant after multiple comparisons correction. Error bars represent standard error of the mean.

Altered striato-cortical connectivity is associated with an array of behavioral disorders involving impulse control problems including cocaine addiction [Hu et al., 2015] and obsessive-compulsive disorder [Beucke et al., 2013; Menzies et al., 2008]. Such connectivity is known to be dopamine-sensitive [Cole et al., 2013]. Thus, we hypothesized that impulsive PD patients would exhibit altered limbic connectivity, especially while on-DAA. The ventral striatum is the target of the mesolimbic pathway

classically implicated in incentivized behavior, response to reward cues, and reward-based learning [Ikemoto and Panksepp, 1999; Olds and Milner, 1954]. DAAs can alleviate motor impairment in PD patients by mimicking endogenous dopamine effects on the dorsal striatum. However, exogenous dopamine also activates the ventral striatum, modifying reward and behavioral circuit activity, including striatal feedback loops serving nonmotor cortical regions [Cools et al., 2001, 2007]. The involvement of the

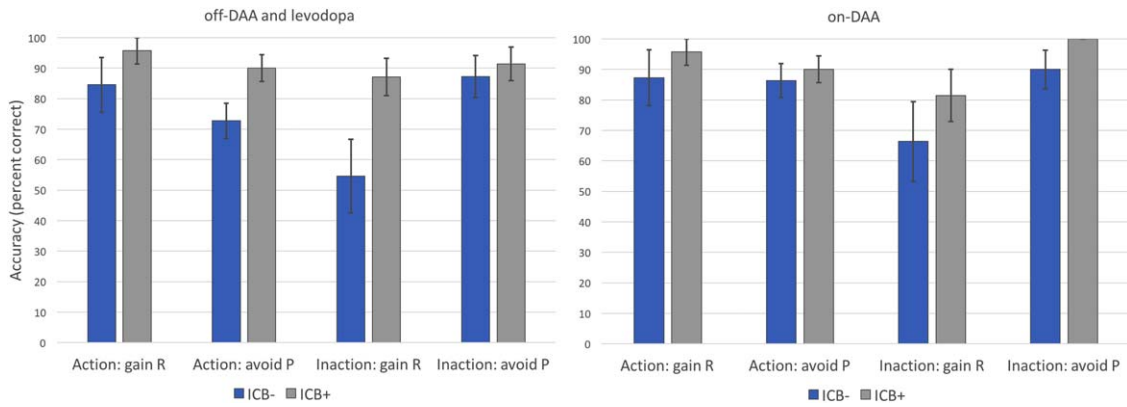


Figure 4.

Action-valence learning scores. Vertical axis represents percentage correct responses. In both off-dopamine and on-DAA conditions, ICB+ outscored ICB- participants in all action-valence pairings. Note: the rightmost condition lacks an error bar because all subjects scored 100% in that condition. “R” indicates reward condition, “P” denotes punishment avoidance. Error bars represent standard error of the mean.

ventral striatum in ICB is substantiated by our finding of increased cerebral blood flow to this structure in ICB+ patients [Claassen et al., 2017].

Carriere et al., 2015 observed altered striato-cortical connectivity in PD-related ICB; however, they identified ICB-related functional disconnection only in the dorsal striatum, especially the putamen. Our results build on these studies and demonstrate the importance of increased ventral striatum connectivity as a correlate and potential driver of ICB. The difference in these findings may be due to the prior study’s inclusion of the ventral caudate and putamen in the ventral striatum seed region, rather than the nucleus accumbens alone, as in our study. Surprisingly, our analysis did not indicate a DAA effect on ventral striatum connectivity. It is thus possible that DAAs act upon pre-existing group differences in connectivity. Alternatively, the absence of a direct drug effect may suggest that the impact of DAA on functional connectivity persists during the 36-h drug wash-out we employed. Future studies with longer off-dopamine periods may resolve this question. Our results nonetheless reveal that elevated connectivity in striatal-limbic cortex

pathways reflects enhanced incentive-based learning and impulse control problems.

Parts of the anterior cingulate gyrus and orbitofrontal cortex participate in a cortico-striatal-pallido-thalamo-cortical loop, one of a series of parallel feedback pathways between the cortex and striatum [Alexander et al., 1986] (Fig. 5A). Unlike other cortical areas which connect via the caudate or putamen, the limbic loop between the basal ganglia and the limbic cortex passes through ventral, rather than dorsal, striatum. Johansen-Berg et al. [2008] used diffusion tensor tractography to evaluate structural connectivity between the nucleus accumbens and the anterior cingulate. Our findings are consistent with functional connectivity between these regions reflecting positively reinforced learning in humans.

Since the ventral striatum-anterior cingulate network is more synchronous in individuals with ICB, and ICB involves heightened sensitivity to reward outcomes and more proficient learning, this suggests a mechanism whereby DAA medication may influence the development of problematic reinforced behaviors. The anterior cingulate

TABLE III. Incentive learning and connectivity LASSO regression results

	Subgenual anterior cingulate	Occipital cortex	Insula	Midbrain	Dorsal anterior cingulate	Caudate	Putamen	Amygdala	Pallidum	Orbitofrontal cortex	Ventromedial prefrontal cortex
Reward learning	91.0†	63.2	54	53	25.2	16.6	16.6	10.4	0.4	0.2	0.2
Punishment learning	30.8	5.8	4.4	22.8	1.8	9.2	1.2	5.4	5.8	63.8	4.4

Values represent the percentage of bootstrapped regressions in which connectivity between ventral striatum and the given ROI was chosen as important for explaining reward or punishment learning. The regression was collapsed across drug states, and controlled for impulse control disorder. Results exceeding 80% are indicated with (†).

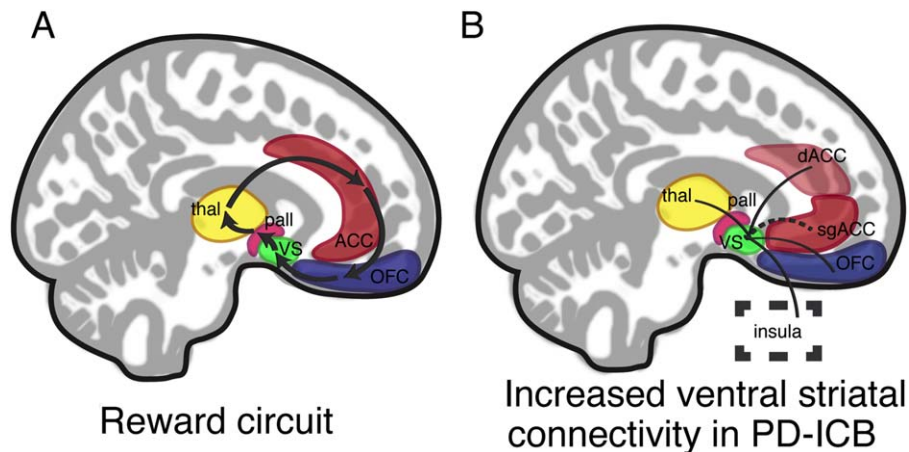


Figure 5.

Schematic representation of the network changes identified in analysis. A, The limbic or affective striato-pallido-thalamo-cortical loop. Arrows represent anatomical connections as described in Alexander et al. [1986]. The loop consists of the ventral striatum (green), the globus pallidus (magenta), the thalamus (yellow), and limbic cortical structures such as the orbitofrontal cortex and anterior cingulate gyrus (red). We propose that this structural and functional network is involved in

is involved in decision-making and outcome evaluation [Bush et al., 2000], and its activity is modulated by expected reward [Amiez et al., 2005]. Moreover, in primates, it has been implicated not only in reward valuation and decision-making [Shima and Tanji, 1998], but in reward learning [Hadland et al., 2003].

Similarly, activity of the orbitofrontal cortex has been linked to both cued and uncued impulsive choices [Zeeb et al., 2010]. Along with the cingulate cortex, it contributes to reward valuation processes, and may mediate hedonic experiences [Dolan, 2007; Kringelbach, 2005]. An important caveat is that the orbitofrontal cortex is prone to signal dropout and geometric distortion in long echo time gradient echo sequences due to its proximity to the sinuses [Deichmann et al., 2002]; this effect can produce spurious results due to signal dropout. The insula is also associated with decision-making and risk evaluation [Bossaerts, 2010; Clark et al., 2008], and is activated when taking risks, especially when the gamble is successful [Xue et al., 2010].

Our results show a pattern of ventral striatal functional involvement with cortical areas known to affect action choice when outcomes are uncertain but potentially rewarding or reinforcing. Based on these data, we propose a model in which DAAs activate ventral striatum $D_{2/3}$ receptor-bearing neurons, leading to increased connectivity in feedback pathways between the ventral striatum and limbic cortex (Fig. 5B). This, in turn, intensifies reward-learning behavior, leading to decision-making that is highly reward-sensitive and hedonic.

incentive valuation and reward-driven behavioral modification. B, Increased functional connectivity correlates of ICB. Bands indicate select regions of significantly increased connectivity, generally corresponding to the cortico-striatal-pallido-thalamo-cortical loop, which is highly connective in ICB+ PD individuals. Dashed connecting line between ventral striatum and subgenual ACC represents functional connectivity related to reward-incentivized learning.

It is important to avoid drawing overly detailed mechanistic conclusions from functional connectivity studies, especially in striatal networks, where inhibitory and excitatory stop-and-go circuits function in parallel in the same space. However, the relationship between the limbic loop and reward-learning argues that our functional connectivity findings mirror basic neuropsychological processes which may help explain the singular behavior of individuals with ICB.

The amygdala, like other limbic system components, has been repeatedly linked to reward-guided learning [Murray, 2007], and one study showed that its effects on reward-based learning vary with the application of D3 agonist [Hitchcott et al., 1997]. The amygdala receives dopaminergic connections from the midbrain [Hyman et al., 2009], and functional and structural connectivity between the two regions has been implicated in feedback-guided learning [Cohen et al., 2008]. Unexpectedly, we found a strong trend toward increased connectivity between these regions in ICB, but only when on-DAA. This indicates a second limbic substrate upon which DAAs may act to promote impulsivity. Further studies are needed to identify how striato-cortical and amygdala-midbrain networks differ in their contributions to impulse control problems.

These findings should also be considered in the context of several limitations. While this study was powered to examine differences in ICB phenotypic groups, it is possible that drug effects on ventral striatal connectivity might

be revealed by a larger sample size. A future study might also examine potential network differences between more risk-related ICB manifestations such as gambling (our study did not include any problem gamblers) and more hedonic variants such as binge eating. Additionally, the performance of the incentive-learning task was limited to a subset of patients ($n = 20$) outside of the scanner. The task was designed to limit the impact of between-session learning by several means, including practice sessions to ensure task familiarity on both study days, and new reward-stimulus associations on the second day to prevent a cumulative learning effect. Nonetheless, we cannot rule out the possibility of some inter-session learning unrelated to drug or ICB group. Another possible limitation of the incentive-learning task is the observation that ICB patients trended toward superior punishment avoidance-learning as well as reward-learning. This suggests that they may be more learning-proficient in general, although we note that punishment-based learning was not found to be strongly related to reward circuit connectivity. Future studies that use a task-based fMRI paradigm may provide insights into acute activity changes experienced by impulsive and compulsive drug-responders when evaluating potential outcomes of risky choices, and adapting behavior to seek rewards. Finally, only BOLD connectivity patterns are reported here, which provide insights with regard to network connectivity differences but limited information on underlying mechanisms. Ongoing work is focused on understanding these findings in the context of dopamine availability and ^{18}F PET studies, cerebral blood flow CBF using arterial spin labeling MRI [Claassen et al., 2017], and neurotransmission using magnetic resonance spectroscopy.

In conclusion, these results illustrate important relationships between reward circuits, D2-like agonists, and behavioral phenotypes in PD. The findings of enhanced connectivity in the striato-pallido-thalamo-cortical network in patients with compulsive reward-driven behaviors has long been biologically suspected, but we can now localize an anatomic network to defined behavioral changes in PD patients. The relationship between connectivity of the ventral striatum and anterior cingulate with improved incentive learning provides important clinical relevance to BOLD findings. Furthermore, the finding that DAA therapy may augment amygdala to midbrain connectivity emphasizes that these key regions, the ventral striatum, cingulate cortex, and amygdala, act together in concert to regulate reward-driven behaviors, where alterations to these connected regions may fundamentally change an individual's ability to regulate comportment.

ACKNOWLEDGMENTS

The authors are grateful to Leslie McIntosh, Claire Jones, Christopher Thompson, Kristen George-Durrett, Charles Nockowski, and Carlos Faraco for experimental support.

CONFLICTS OF INTEREST

The authors declare no relevant conflicts of interest.

REFERENCES

- Alexander GE, DeLong MR, Strick PL (1986): Parallel organization of functionally segregated circuits linking basal ganglia and cortex. *Annu Rev Neurosci* 9:357–381.
- American Psychiatric Association (2013): DSM-V. Arlington, VA: American Journal of Psychiatry.
- Amiez C, Joseph J-P, Procyk E (2005): Anterior cingulate error-related activity is modulated by predicted reward. *Eur J Neurosci* 21:3447–3452.
- Behzadi Y, Restom K, Liu J, Liu TT (2007): A component based noise correction method (CompCor) for BOLD and perfusion based fMRI. *Neuroimage* 37:90–101.
- Benjamini Y, Hochberg Y (1995): Controlling the false discovery rate: A practical and powerful approach to multiple testing. *J R Stat Soc B* 57:289–300.
- Beucke JC, Sepulcre J, Talukdar T, Linnman C, Zschenderlein K, Endrass T, Kaufmann C, Kathmann N (2013): Abnormally High Degree Connectivity of the Orbitofrontal Cortex in Obsessive-Compulsive Disorder. *JAMA Psychiatry* 70:619.
- Bogacz R, Gurney K (2007): The Basal Ganglia and Cortex Implement Optimal Decision Making Between Alternative Actions. *Neural Comput* 19:442–477.
- Bossaerts P (2010): Risk and risk prediction error signals in anterior insula. *Brain Struct Funct* 214:645–653.
- Bush G, Luu P, Posner MI (2000): Cognitive and emotional influences in anterior cingulate cortex. *Trends Cogn Sci* 4:215–222.
- Cador M, Robbins TW, Everitt BJ (1989): Involvement of the amygdala in stimulus-reward associations: Interaction with the ventral striatum. *Neuroscience* 30:77–86.
- Carriere N, Lopes R, Defebvre L, Delmaire C, Dujardin K (2015): Impaired corticostriatal connectivity in impulse control disorders in Parkinson disease. *Neurology* 84:2116–2123.
- Cherubini A, Péran P, Caltagirone C, Sabatini U, Spalletta G (2009): Aging of subcortical nuclei: Microstructural, mineralization and atrophy modifications measured in vivo using MRI. *Neuroimage* 48:29–36.
- Claassen DO, Stark AJ, Spears CA, Petersen KJ, van Wouwe N, Kessler R, Zald D, Donahue M: Mesocorticolimbic hemodynamic response in Parkinson's disease patients with compulsive behaviors. *Mov Disord* doi:10.1002/mds.27047.
- Clark L, Bechara A, Damasio H, Aitken MRF, Sahakian BJ, Robbins TW (2008): Differential effects of insular and ventromedial prefrontal cortex lesions on risky decision-making. *Brain* 131:1311–1322.
- Cohen MX, Elger CE, Weber B (2008): Amygdala tractography predicts functional connectivity and learning during feedback-guided decision-making. *Neuroimage* 39:1396–1407.
- Cole DM, Oei NYL, Soeter RP, Both S, Van Gerven JMA, Rombouts SAR, Beckmann CF (2013): Dopamine-dependent architecture of cortico-subcortical network connectivity. *Cereb Cortex* 23:1509–1516.
- Cools R, Barker RA, Sahakian BJ, Robbins TW (2001): Enhanced or Impaired Cognitive Function in Parkinson's Disease as a Function of Dopaminergic Medication and Task Demands. *Cereb Cortex* 11:1136–1143.
- Cools R, Lewis SJG, Clark L, Barker RA, Robbins TW (2007): L-DOPA Disrupts Activity in the Nucleus Accumbens during

- Reversal Learning in Parkinson's Disease. *Neuropsychopharmacology* 32:180–189.
- Dagher A, Robbins TW (2009): Personality, Addiction, Dopamine: Insights from Parkinson's Disease. *Neuron* 61:502–510.
- Deichmann R, Josephs O, Hutton C, Corfield DR, Turner R (2002): Compensation of Susceptibility-Induced BOLD Sensitivity Losses in Echo-Planar fMRI Imaging. *Neuroimage* 15:120–135.
- Dolan R (2007): The human amygdala and orbital prefrontal cortex in behavioural regulation. *Philos Trans R Soc B Biol Sci* 362:787–799.
- Friedman J, Hastie T, Tibshirani R (2010): Regularization Paths for Generalized Linear Models via Coordinate Descent. *J Stat Softw* 33:1–22.
- Genovese CR, Lazar NA, Nichols T (2002): Thresholding of Statistical Maps in Functional Neuroimaging Using the False Discovery Rate. *Neuroimage* 15:870–878.
- Goetz CG, Tilley BC, Shaftman SR, Stebbins GT, Fahn S, Martinez-Martin P, Poewe W, Sampaio C, Stern MB, Dodel R, Dubois B, Holloway R, Jankovic J, Kulisevsky J, Lang AE, Lees A, Leurgans S, LeWitt PA, Nyenhuis D, Olanow CW, Rascol O, Schrag A, Teresi JA, van Hilten JJ, LaPelle N, Agarwal P, Athar S, Bordelan Y, Bronte-Stewart HM, Camicioli R, Chou K, Cole W, Dalvi A, Delgado H, Diamond A, Dick JP, Duda J, Elble RJ, Evans C, Evidente VG, Fernandez HH, Fox S, Friedman JH, Fross RD, Gallagher D, Goetz CG, Hall D, Hermanowicz N, Hinson V, Horn S, Hurtig H, Kang UJ, Kleiner FG, Klepitskaya O, Kompoliti K, Lai EC, Leehey ML, Leroi I, Lyons KE, McClain T, Metzger SW, Miyasaki J, Morgan JC, Nance M, Nemeth J, Pahwa R, Parashos SA, Schneider JSJS, Schrag A, Sethi K, Shulman LM, Siderowf A, Silverdale M, Simuni T, Stacy M, Stern MB, Stewart RM, Sullivan K, Swope DM, Wadia PM, Walker RWR, Walker RWR, Weiner WJ, Wiener J, Wilkinson J, Wojcieszek JM, Wolfrath S, Wooten F, Wu A, Zesiewicz TA, Zweig RM (2008): Movement Disorder Society-Sponsored Revision of the Unified Parkinson's Disease Rating Scale (MDS-UPDRS): Scale presentation and clinimetric testing results. *Mov Disord* 23:2129–2170.
- Haber SN, Behrens TE (2014): The Neural Network Underlying Incentive-Based Learning: Implications for Interpreting Circuit Disruptions in Psychiatric Disorders. *Neuron* 83(5):1019–1039.
- Hadland KA, Rushworth MFS, Gaffan D, Passingham RE (2003): The anterior cingulate and reward-guided selection of actions. *J Neurophysiol* 89:1161–1164.
- Hitchcott PK, Bonardi CMT, Phillips GD (1997): Enhanced stimulus-reward learning by intra-amygdala administration of a D3 dopamine receptor agonist. *Psychopharmacology (Berl)* 133:240–248.
- Hu Y, Salmeron BJ, Gu H, Stein EA, Yang Y (2015): Impaired Functional Connectivity Within and Between Frontostriatal Circuits and Its Association With Compulsive Drug Use and Trait Impulsivity in Cocaine Addiction. *JAMA Psychiatry* 72: 584.
- Hyman S, Sydor A, Brown R, Malenka R, Nestler E (2009): Molecular Neuropharmacology: A Foundation for Clinical Neuroscience, 2nd ed. New York: McGraw-Hill. pp 265–266.
- Ikemoto S, Panksepp J (1999): The role of nucleus accumbens dopamine in motivated behavior: A unifying interpretation with special reference to reward-seeking. *Brain Res Rev* 31: 6–41.
- Johansen-Berg H, Gutman DA, Behrens TEJ, Matthews PM, Rushworth MFS, Katz E, Lozano AM, Mayberg HS (2008): Anatomical connectivity of the subgenual cingulate region targeted with deep brain stimulation for treatment-resistant depression. *Cereb Cortex* 18:1374–1383.
- Kringelbach ML (2005): The human orbitofrontal cortex: linking reward to hedonic experience. *Nat Rev Neurosci* 6:691–702.
- Maldjian J (1994): WFU PickAtlas User Manual v2. 4. *Hum Brain Mapp* 63:1–13.
- Menzies L, Chamberlain SR, Laird AR, Thelen SM, Sahakian BJ, Bullmore ET (2008): Integrating evidence from neuroimaging and neuropsychological studies of obsessive-compulsive disorder: The orbitofronto-striatal model revisited. *Neurosci Biobehav Rev* 32:525–549.
- Murray AM, Ryoo HL, Gurevich E, Joyce JN (1994): Localization of dopamine D3 receptors to mesolimbic and D2 receptors to mesostriatal regions of human forebrain. *Proc Natl Acad Sci U S A* 91:11271–11275.
- Murray EA (2007): The amygdala, reward and emotion. *Trends Cogn Sci* 11:489–497.
- Olds J, Milner P (1954): Positive reinforcement produced by electrical stimulation of septal area and other regions of rat brain. *J Comp Physiol Psychol* 47:419–427.
- Patenaude B, Smith SM, Kennedy DN, Jenkinson M (2011): A Bayesian model of shape and appearance for subcortical brain segmentation. *Neuroimage* 56:907–922.
- Perez-Lloret S, Rey MV, Fabre N, Ory F, Spampinato U, Montastruc J-L, Rascol O (2011): Impulse-control disorders in Parkinson's disease patients. *Eur J Neurol* 18:483.
- Pierce RC, Kumaresan V (2006): The mesolimbic dopamine system: The final common pathway for the reinforcing effect of drugs of abuse? *Neurosci Biobehav Rev* 30:215–238.
- Shima K, Tanji J (1998): Role for cingulate motor area cells in voluntary movement selection based on reward. *Science* 282: 1335–1338.
- Smith SM, Jenkinson M, Woolrich MW, Beckmann CF, Behrens TEJ, Johansen-Berg H, Bannister PR, De Luca M, Drobnjak I, Flitney DE, Niazy RK, Saunders J, Vickers J, Zhang Y, De Stefano N, Brady JM, Matthews PM (2004): Advances in functional and structural MR image analysis and implementation as FSL. *Neuroimage* 23:S208–S219.
- Smith SM, Fox PT, Miller KL, Glahn DC, Fox PM, Mackay CE, Filippini N, Watkins KE, Toro R, Laird AR, Beckmann CF (2009): Correspondence of the brain's functional architecture during activation and rest. *Proc Natl Acad Sci* 106:13040–13045.
- Tanaka SC, Doya K, Okada G, Ueda K, Okamoto Y, Yamawaki S (2004): Prediction of immediate and future rewards differentially recruits cortico-basal ganglia loops. *Nat Neurosci* 7: 887–893.
- Tibshirani R (1996): Regression Selection and Shrinkage via the Lasso. *J R Stat Soc B* 58:267–288.
- Tomlinson CL, Stowe R, Patel S, Rick C, Gray R, Clarke CE (2010): Systematic review of levodopa dose equivalency reporting in Parkinson's disease. *Mov Disord* 25:2649–2653.
- Tye KM, Stuber GD, de Ridder B, Bonci A, Janak PH (2008): Rapid strengthening of thalamo-amygdala synapses mediates cue-reward learning. *Nature* 453:1253–1257.
- Voon V, Fox SH (2007): Medication-Related Impulse Control and Repetitive Behaviors in Parkinson Disease. *Arch Neurol* 64:1089.
- Weintraub D (2009): Impulse control disorders in Parkinson's disease: prevalence and possible risk factors. *Parkinsonism Relat Disord* 15: S110–S113.
- Weintraub D, David AS, Evans AH, Grant JE, Stacy M (2015): Clinical spectrum of impulse control disorders in Parkinson's disease. *Mov Disord* 30:121–127.

- Van Wouwe NC, Claassen DO, Neimat JS, Kanoff KE, Wylie SA (2017): Dopamine Selectively Modulates the Outcome of Learning Unnatural Action–Valence Associations. *J Cogn Neurosci* 29:816–826.
- Xue G, Lu Z, Levin IP, Bechara A (2010): The impact of prior risk experiences on subsequent risky decision-making: The role of the insula. *Neuroimage* 50:709–716.
- Zeeb FD, Floresco SB, Winstanley CA (2010): Contributions of the orbitofrontal cortex to impulsive choice: Interactions with basal levels of impulsivity, dopamine signalling, and reward-related cues. *Psychopharmacology (Berl)* 211:87–98.
- Zhang Y, Zhang J, Xu J, Wu X, Zhang Y, Feng H, Wang J, Jiang T (2014): Cortical gyrification reductions and subcortical atrophy in Parkinson’s disease. *Mov Disord* 29:122–126.